# A Virtual Brain Model to examine the effects of critical brain dynamics on pre-stimulus phase and amplitude regulation

**Peixuan Wu**[1,*], **Additya Sharma**[1], **and Klaus Linkenkaer-Hansen**[1]

[1]Department of Integrative Neurophysiology (INF), Center for Neurogenomics and Cognitive Research (CNCR), Amsterdam Neuroscience, Amsterdam, Netherlands
[*]p.peixuan@student.vu.nl

## ABSTRACT

The excitatory/inhibitory balance (E/I balance) is crucial to the function of the brain. Previous simulation studies have shown that the neuronal networks under E/I balance,which is considered as critical state, exhibits the largest modulation effect in response to a stimulation. In order to examine the generality of the discovery, a model based on the Wilson-Cowan model was built using The Virtual Brain. By tuning the E/I ratio, the model can exhibit a high and low exponent in detrended fluctuation analysis, which may imply near-critical and non-critical states. We find that the level of pre-stimulus regulation depends on the number of stimulated neurons. The critical networks exhibit a higher range of pre-stimulus regulation when a large number of neurons are stimulated. The study confirms the relationship between criticality and versality of modulation in stimulus processing.

## Introduction

A balanced excitatory and inhibitory synaptic connectivity in the brain plays an important role in visual perception[1]. A balanced excitatory/inhibitory connectivity ratio (E/I ratio) is considered to manifest a transient state between chaotic and order. Hypothetically, the so-called critical state allows the neural system to exhibit coupling and variability and attains the maximum efficiency in computation as well as the information propagation[2].

Mathematically, the dynamics of the critical system follow the power-law, which means the probability distribution of a certain property x is in the form of $p(x) = Cx^{-a}$[3]. Power-law distribution is also called scale-free distribution, implying that the property exhibits a pattern presented on all the scales. Criticality has been observed in electroencephalography (EEG) recordings, in which the distribution of the signal amplitude follows the power-law. By employing the detrended fluctuation analysis (DFA), the temporal structure of the brain oscillations is characterized by a decaying autocorrelation called long-range temporal correlations (LRTCs)[4]. Within all the rhythms, alpha oscillation (8-14Hz) is one of the candidate mechanisms for conscious perception. EEG recordings have shown that the power of alpha oscillations decrease in task-related regions, but increase in disengaged regions[5]. The popular view considers alpha oscillation as a top-down control mechanism which gates the information that the brain needs to focus on.

In order to investigate the role of criticality in perception, Avramiea et al. simulated the critical state with a model of criticality oscillations (CROS)[6]. The model contains 50x50 neurons where 75% are excitatory and 25% are inhibitory. Networks are created by adjusting the E/I ratio of the model. By computing the DFA for the alpha-band oscillations, the networks are categorized into sub-critical, critical, and super-critical states based on the E/I ratio as well as LRTCs. The study showed that the networks under critical state exhibit the largest extent of regulatory effect in response to a stimulation. Phase-locking factor (PLF) across the trials of stimulation is used to measure the uniformity of stimulus response. Among the three critical states, networks in critical state show maximum dynamic ranges in response to a single-pulse stimulation. The amplitude and phase angle before the stimulation exhibit highest regulatory effect to the PLF.

The result above has shown that criticality is an optimal state for a neuronal network to respond to a stimulation. Nevertheless, the study is based on the assumption of homogeneous neurons and neglecting anatomic details but only preserves the key properties of a neuronal network.

To address the potential problem of oversimplification, a possible solution is to investigate the criticality in a more biologically plausible model using The Virtual Brain. TVB is a system-level simulation of the human brain[7]. TVB could combine both region-based and surface-based modeling to create an integrated model with a flexible detail setting. In the region-based modeling, TVB simulates the neuronal dynamics of mesoscale regions basing on the tractography connectome. On the basis of region-based modeling, surface-based modeling provides a fine-grained modeling for the subpopulation within cortical regions. Different modalities including EEG, magnetoencephalography , and functional Magnetic Resonance Imaging are provided as outputs of the neuronal dynamics. In addition, TVB provides connectome specification, stimulation application, and time series analysis toolbox. The platform provides a powerful tool to simulate brain dynamics with anatomical and functional detail. Recently, TVB has been integrated into the digital infrastructure EBRAINS[8], which enables the researchers to get access to computation and storage resources. The examination of the model could help us investigate the generality of the previous study on pre-stimulus regulation by Avramiea et al[6].

The aim of this study is to reinvestigate the pre-stimulus regulation of criticality using the model built on TVB. A model was optimized to exhibit E/I dependent critical dynamics. By analyzing the signal produced by the model, we found that the level of pre-stimulus regulation depends on the number of simulated neurons. Though the regulatory behavior is inconsistent with the previous study, the critical networks still exhibit higher level of pre-stimulus regulation when a large number of neurons are stimulated.

## Results

### A neural field model producing critical and noncritical states

In this paper, we simulated the brain signal on a triangulated surface of the primary visual cortex in the left hemisphere with 177 vertices (Fig.1a). Each vertex represents a neuronal population on the scale of millimeters. For each vertex, the dynamics of the average firing rate is defined with a Wilson-Cowan (WC) model[9] The model (see Methods – Neural field model and Fig.1b) consists of excitatory and inhibitory populations. The populations not only are mutually connect to each other (with weight defined as $W_{EI}$ and $W_{IE}$), but also has an internal connection (with weight $W_{EE}$ and $W_{II}$) and receive excitatory and inhibitory input from other vertices. In order to introduce stochastic characteristics to the system, a multiplicative noise was added for each step of numerical integration.[10] The output of the model is the average firing rate of the excitatory population across all the vertices.

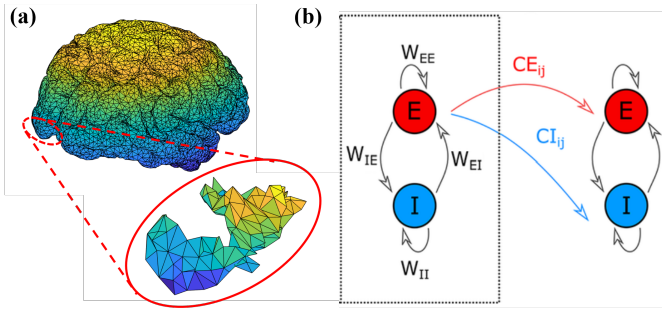


**Figure 1.** An illustration of the model **a)** The model is based on a triangulated surface of the primary visual cortex in the left hemisphere with 177 vertices. The dynamic of each vertex is simulated by a WC model. **b)** In WC model,each vertex is composed of excitatory (E) and inhibitory (I) subpopulations. For each time step, a population receives input signal from its counterparts (whose connectivity weight is denoted by $W_{EI}$ or $W_{IE}$) also neurons within itself (whose connectivity weight is denoted by $W_{EE}$ and $W_{II}$). The populations couple inputs from other vertices as well, which is demoted by $CE_{ij}$ or $CI_{ij}$. Adapted from paper by Lea-Carnall[11]

We first optimized the model to exhibit critical dynamics. In order to refine the parameter to be tuned, the parameter space was first explored by visualizing the phase plane of the model. The parameter set was manually adjusted to give a fixed point or limit cycle in the phase plane, whose outputs are able to exhibit bursts or oscillations under the stochastic integration scheme. Next, the refined parameter set was used as input, which is further optimized by Bayesian optimization to a critical state.

During the optimization, the critical state is characterized by the DFA exponent (Fig.2). The signal was filtered by delta, theta, alpha, beta, and gamma bands. Considering that the scale-free property may exhibit in throughout the scale of frequency

domain, not only the DFA exponent of filtered signal, but also raw signal is computed. We tried to produce a DFA exponent above 0.75 in alpha oscillation, which is close to the DFA exponent of alpha band from EEG recording of the healthy control[12]. To do so, the power spectrum density was also computed (Fig.2 g-l). Whether the network produces alpha oscillations was counted into penalty during the optimization. Eventually, the model was optimized to generate signals with DFA exponent above 0.75 in the delta band but did not produce a prominent oscillation in any band (Fig.2 g).

In order to examine whether the model is able to exhibit various critical dynamics, the E/I ratio of the model was tuned in a grid space. The grid space is defined by spanning both the weight of the excitatory-excitatory population ($W_{EE}$) and the inhibitory-excitatory population ($W_{EI}$) ranging from 6 to 22 with a step of 4 and fixing all the other parameters. The DFA exponent in the delta band gradually changes in the grid space, ranging from 0.5-0.8. However, the model can only manifest critical and noncritical states, since the DFA exponent of super-critical (higher E/I ratio) and critical states are hardly distinguishable. On the other hand, the DFA exponents of the model in other bands, such as the alpha band, keep around 0.5 in the whole grid space (Fig.3a, b).

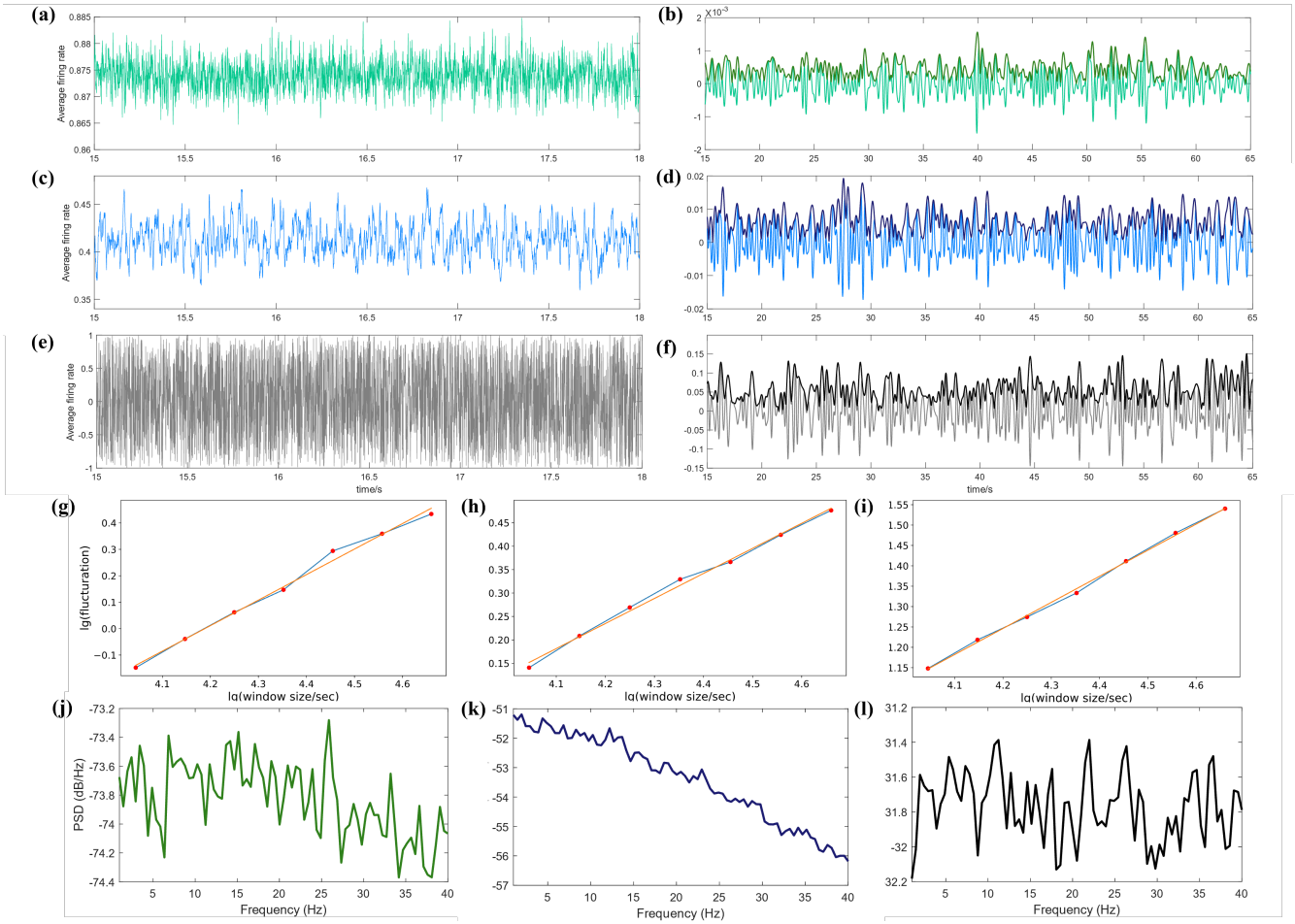


**Figure 2.** An example of detrended fluctuation analysis (DFA). **a)** Signals simulated by the model with a balanced E/I ratio. **b)** Signals simulated by the model with a low E/I ratio **c)** Signals generated randomly by the uniform distribution. Main parameters of the network: Near-critical: $W_{EE} = 11.57$, $W_{IE} = 10.31$; Near-critical: $W_{EE} = 6$, $W_{IE} = 22$. The following analysis is carried on the two representative network. **b, d, f)** The signals were filtered in delta band (0.5-4Hz) and the amplitude envelope were was extracted (bold lines in deeper colors). **g, h, i)** The cumulative sum of the signal was computed from the amplitude envelope and then was detrended to generate the signal profile. The fluctuation is computed from a series of standard deviation were computed by varying the time window. DFA exponents are computed by linear regression to the logarithmic scales of fluctuation and window sizes. The DFA exponent in g): 0.77, $R^2$=0.9926; h): 0.54, $R^2$=0.9953; i): 0.54, $R^2$=0.9960. **j, k, l)** The power spectrum density of the three signals.

### Phase-locking factor as a measurement of stimulus response

In order to investigate how the network responds to stimulation in critical and non-critical states, a single pulse stimulus lasting for 1 time step (1ms) with a fixed strength is applied to n random vertex on the surface. Stimulation size is defined by the number of vertices that are stimulated.

External stimulation will cause a reset in the phase of the neuronal oscillation.[13] A few previous studies used amplitude changes as a measurement of the dynamic range. However, the fluctuating nature of the amplitude will potentially affect the analysis of amplitude changing after stimulation. Therefore, here, we observe the phase-locking response after applying stimulation to the network. To measure the uniformity of phase-locking response, phase-locking factor (PLF), is defined by the average phase of an oscillation at a time point after the stimulation across trials. We found that the reset effect to the phase is related to the stimulation size. The more neurons are stimulated, the more possibility of the phase aligning to the stimulation. Consistent with previous research[6], simulation shows that the critical signal has a higher dynamic range of PLF than the non-critical network (Fig.3c).

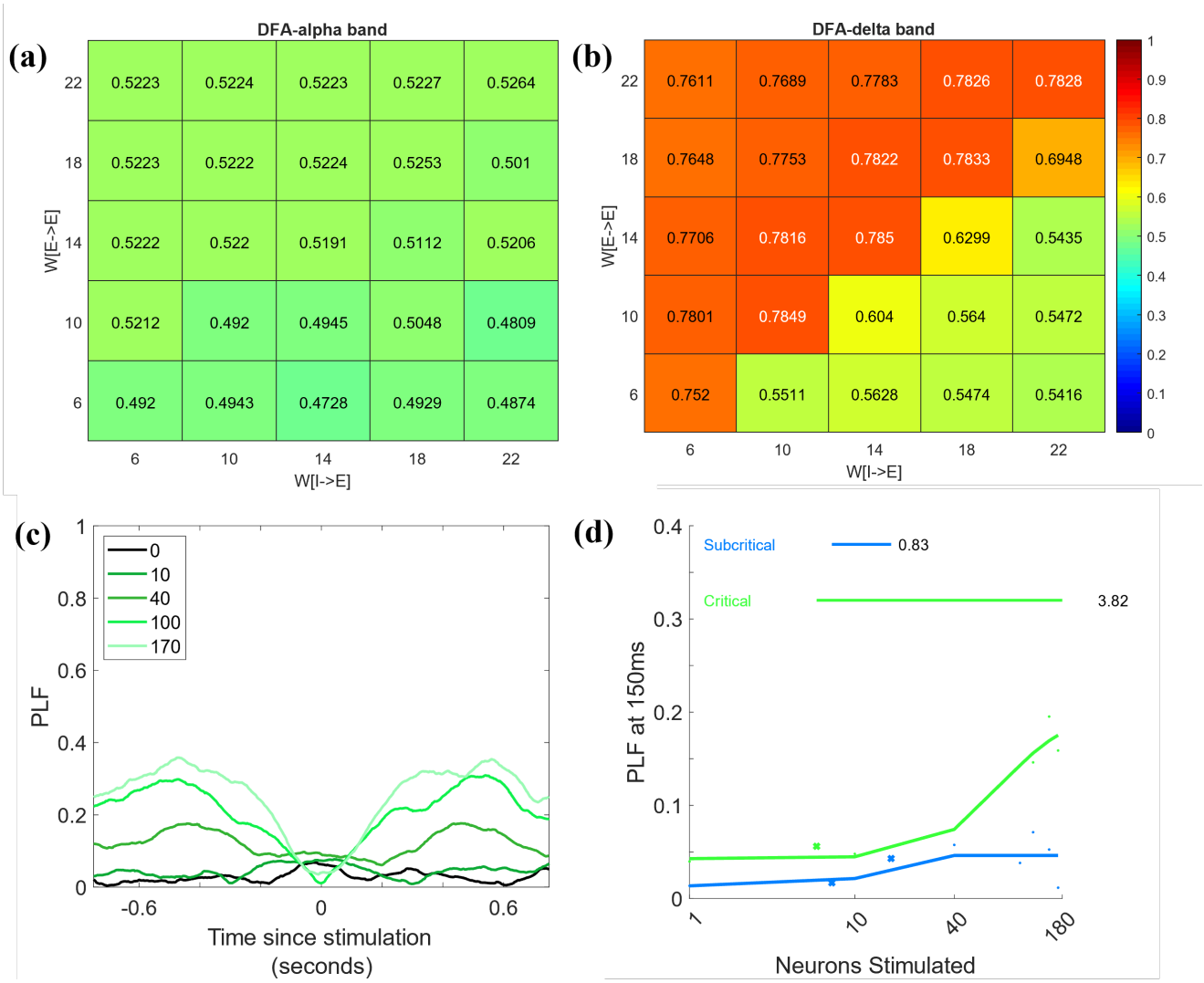


**Figure 3.** The critical network shows a large dynamic range than the non-critical network. **a)** The DFA exponent in the alpha band. **b)** The DFA exponent in the delta band. **c)** The phase of the critical signal. 0 is the onset of the stimulation. **d)** The dynamic range of PLF at 150ms after stimulation. Stimulation size is plotted on a natural logarithmic scale. Sigmoid is used to fit the curve. The dynamic range is defined by the natural logarithm of the stimulation size between 10% and 90% of the sigmoid fitting.

## Critical network shows higher level of Pre-stimulus regulation

Having observed a larger dynamic range in the critical network, we asked whether the states before the stimulation relates to the dynamic range of the PLF. We measured the phase and amplitude of the signal 150-50 ms before the stimulation.

We first computed the regulatory effect of pre-stimulus amplitude. We investigated the average amplitude from -150 to -50 ms for each trial and sort them by percentile (Fig.4b, e). We defined the amplitude regulation as the Spearman correlation between the amplitude percentile and PLF at 150ms after stimulation. The PLF at 150ms positively correlates to the amplitude percentile in the critical network, while the non-critical network shows a negative but less prominent regulatory effect. Also, we found that the amplitude regulation depends on the stimulation size. The trend of amplitude regulation is contradictory to previous research. Nevertheless, the amplitude regulation of a critical network is generally more prominent than of the non-critical network (Fig.4).

A similar effect could also be observed in the pre-stimulus phase (see *Methods - Pre-stimulus regulation*). Pre-stimulus phase regulation indicates the relationship between the pre-stimulus phase and PLF after the stimulation. Ranging from 0 to 1, a higher value indicates a higher level of regulation. The result demonstrates that the pre-stimulus phase regulation varies depending on the stimulation size. When the stimulation size is high, the critical network shows more regulatory effect (Fig.5). In contrast to the result of previous research[6], the relationship between the regulation and stimulation size is linear instead of log-linear.

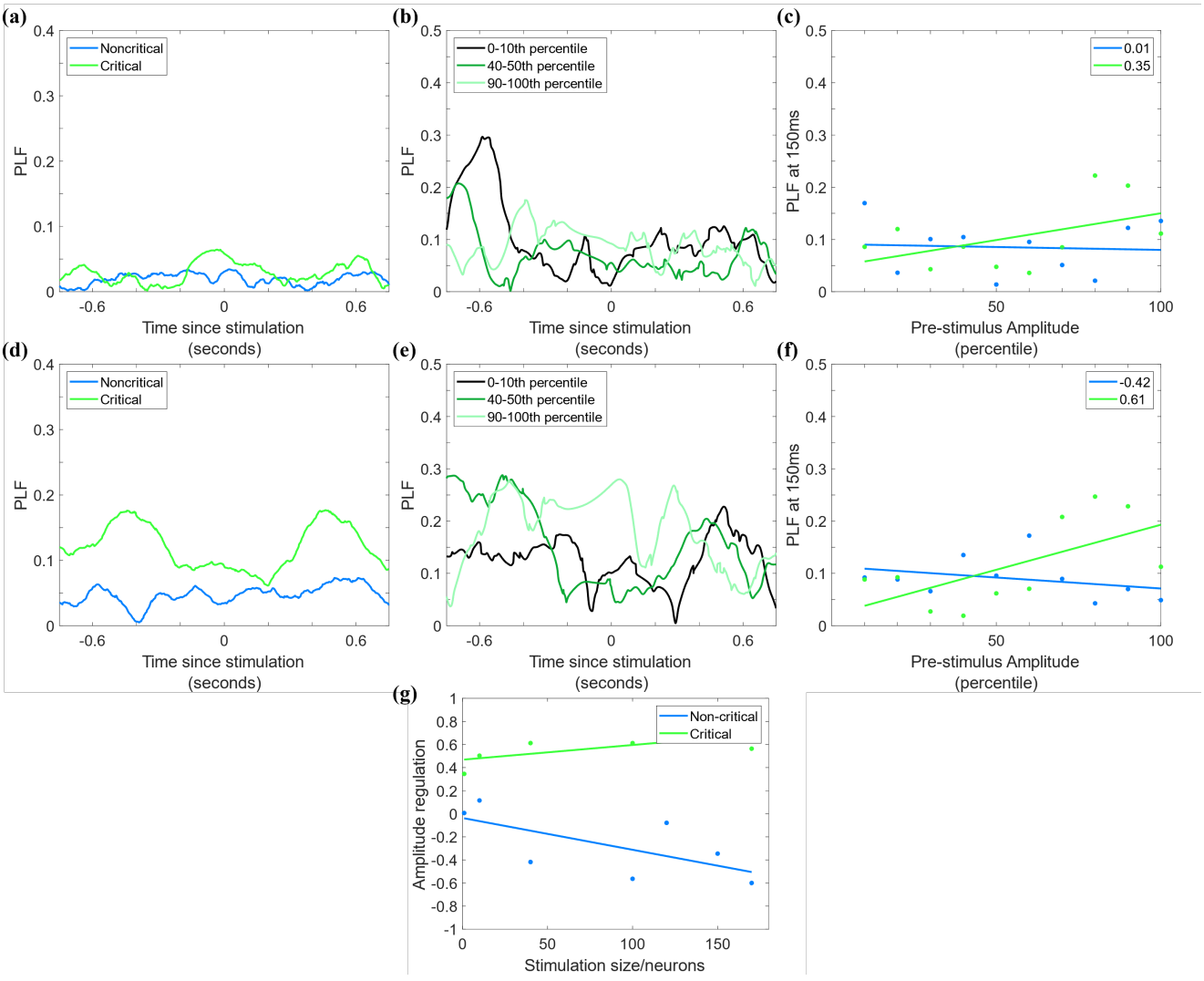

**Figure 4.** The critical network shows a high level of pre-stimulus amplitude regulation than the non-critical network. **a)** The PLF in time series when 1 vertex is stimulated. 0 represents the onset of the stimulation. **b)** Trials are sorted by the percentile of the average pre-stimulus amplitude when a stimulus is applied on 1 vertex. 0 represents the onset of a stimulation. **c)** The relationship between the percentile of pre-stimulus amplitude and PLF at 150ms, when a stimulus is applied on 1 vertex. The number at the top-right indicates the Spearman correlation. **d)** The PLF in time series when 10 vertices are stimulated. **e)** Trials are sorted by the percentile of the average pre-stimulus amplitude when stimuli are applied on 10 vertices. 0 represents the onset of a stimulus. **f)** The relationship between the percentile of pre-stimulus amplitude and PLF at 150ms, when stimuli are applied on 10 vertices. **g)** The relationship between amplitude regulation and stimulation size. $R^2$ for the linear fitting: Non-critical: 0.4332; Critical: 0.4933.

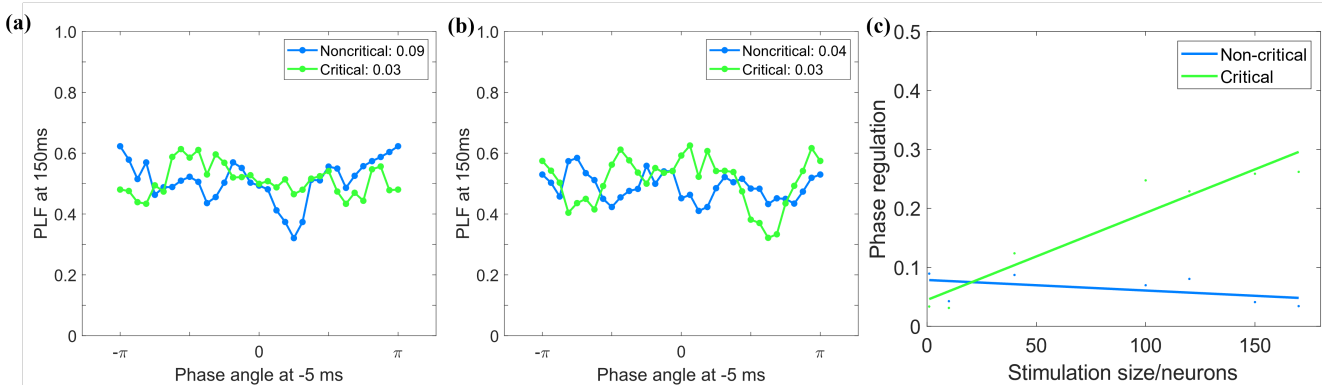


**Figure 5.** The critical network shows a higher level of pre-stimulus phase regulation than the non-critical network. **a)** The relation between PLF and pre-stimulus phase at -5ms, when 10 vertices are stimulated. **b)** The relation between PLF and pre-stimulus phase at -5ms, when 10 vertices are stimulated. **c)** The phase regulation and stimulation size exhibit linear relationship, especially in critical network. $R^2$ for the linear fitting: Non-critical: 0.2636; Critical: 0.9955.

## Discussion

In this study, we attempted to replicate the result that was found in the CROS model[6] on another simulation platform The Virtual Brain. We built a model based on WC model. The model exhibits critical and non-critical dynamics when adjusting E/I ratio. Previous theoretical and simulation works[14–16] have suggested a hypothesis that the critical dynamics in the brain might maximize the dynamic range and optimize information processing. Comparing with the non-critical network, the critical network on TVB shows a higher dynamic range in phase-locking factor, which confirms the critical hypothesis. By comparing the two networks, we investigated the pre-stimulation regulation to the stimulation response. We found that the pre-stimulus amplitude positively regulates the phase-locking factor after the in the critical network, while the CROS model in the critical state shows a negative pre-stimulus amplitude regulation[6]. Despite the inconsistency, the critical network generally shows more prominent pre-stimulus amplitude and phase regulations to PLF after the stimulation.

It's important to note that there're some differences between the methods in the research of Avramiea et al. on CROS model[6] and this paper. First, Avramiea et al. uses integrate-and-fire model where each simulation unit in the model represents a single neuron in the brain, while we use WC model where each simulation unit represents a neuronal population within a brain region. Therefore, there're a smaller number of vertex than CROS model. However, we couldn't establish an equivalent relationship between the two models mathematically. A plausible way to build up two comparable models would be to adjust the parameter of the models using same training dataset that collected from experiment. Second, instead of using neuronal avalanche as an criteria of criticality as the former paper, we use DFA as a criteria.

There are some inconsistencies between the result from our model and CROS model. This might be because we followed the temporal interval between each trials of stimulation and the time constant of analysis protocol of of Avramiea et al.[6] without adjusting it for the delta band. For example, the stimulation time interval and the time point of post-stimulus PLF to be analyzed should be longer than the protocol for alpha oscillations since delta oscillations are much slower. Besides, the result s from our model are still preliminary. Instead of comparing two networks, a more systematic investigation of the regulatory effect should be done by adjusting the E/I ratio in a gradient scale.

One of the main limitations of our research is that our model could only simulate LRTCs in the delta band, but dose not exhibit any other characteristic of an EEG signal of a healthy subject, such as oscillations in a specific band or beta bursts[10]. However, such a limited model happens to prove that critical dynamics on a specific band is necessary and adequate for the network to exhibit a higher level of pre-stimulus regulation within this band. Our model adopts a distinct structure and model for dynamic simulation from CROS model, which suggests that the pre-stimulus regulation might be a generic property of critical systems. However, a stricter proof of the generalization is needed.

We should note that our model only simulates an instance of the brain dynamics. Physiologically, brain networks are always changeable. Each time the brain performs a task, the learning effect might change the network structure gradually by neuronal modulation[17]. With a set of fixed parameters, we can only simulate an instant state of the brain. In the future, a potential study could integrate the task-dependent manner and the learning effect to the network and investigate the evolution of critical dynamics as the network evolves. Our TVB model shows that a network with critical dynamics in delta band also exhibits pre-stimulus regulation to the stimulation response. Previously, some studies have suggested that delta band is prominent in visual cortex during the Silent Lip Reading or attentional selection task when visual and auditory stimulation are coupling[18,19]. Considering the difference in the stimulation scheme and the setting of the model, our investigation on the regulatory effect of delta band oscillations are not in line with this research directly, but it would be interesting to investigate the role of critical dynamics in a visuoauditory modulation task in the future. In this research, we simulated the neuronal dynamics locally within the primary visual cortex on the left hemisphere. TVB is a powerful platform to perform larger scale simulations across multiple brain regions[20,21]. Therefore, taking the advantage of TVB to investigate the role of criticality in information propagation from primary visual cortex to other regions of the brain could be another potential direction for future investigation. Overall, though some of the results are inconsistent with the previous research, our research highlights the function of critical dynamics in regulation of the stimulation response.

## Methods

### Neural field model

The model is designed on a triangulated primary visual cortex surface on the left hemisphere. The surface is trimmed from the default surface of TVB containing 16384 vertices. Within a population, the firing rate of an excitatory or inhibitory subpopulation $\dot{E}$ and $\dot{I}$ were defined separately. The differential equation of the neural dynamics used in The Virtual Brain is adopted from Wilson, H. R. Cowan, J. D[9]:

$$\dot{E}_k = \frac{1}{\tau_e}(-E_k + (k_e - r_e E_k)s_e, \tag{1}$$

$$\dot{I}_k = \frac{1}{\tau_i}(-I_k + (k_i - r_i I_k)s_i, \tag{2}$$

where $r_e$ and $r_i$ are refractory constant; $s_e$ and $s_i$ is response function indicating the integration of the input.

$$s_e = \sigma_e(\alpha_e\left(c_{ee}E_k - c_{ei}I_k + P_k - \theta_e + W_\zeta \cdot E_j + W_\zeta \cdot I_j\right))), \tag{3}$$

$$s_i = \sigma_i(\alpha_i\left(c_{ie}E_k - c_{ee}I_k + Q_k - \theta_i\right) + W_\zeta \cdot E_j + W_\zeta \cdot I_j\right))), \tag{4}$$

where $\sigma_e$ and $\sigma_i$ are sigmoid function; $P$ and $Q$ are constant, which could be considered as excitatory and inhibitory stimulation; $W_\zeta \cdot E_j$ and $W_\zeta \cdot I_j$ are local coupling from other vertices.

The numerical simulation of the differential equation is integrated by Stochastic Heun integrator:

$$X_i(t) = X_i(t-1) + dX(X_i(t)/2 + dX(X_i(t-1)))dt + \varepsilon + \pi dt \tag{5}$$

$X_i$ is state variable $E$ or $I$. Each time step $dt$ of the integration is 1ms. $\pi$ is stimulation. $\varepsilon$ is noise scheme, in which we used a multiplicative Gaussian noise:

$$\sigma = \omega(\sqrt{2 * D} * (\exp(-(X_i^2/(0.6^2)))) + 1) \tag{6}$$

$\omega$ is a random number generated from a normal distribution. $D$ is the standard deviation of the noise, which is considered as a hyperparameter to be optimized. $X_i$ is state variable $E$ or $I$.

The output of the model is the regional average firing rate among all the vertices on V1. The sampling frequency of the recorded signal is 1Hz. For each network, the signal is simulated for 1000 seconds.

### Data preprocess and prilimiary analysis

The Power Spectral Density is computed with Python package Scipy using the Welch method with a Hamming window with 2048 FFT points.

The signal is filtered by the filter from the Python package MNE with the default setting.

The DFA exponent is computed with Python package NBT2 using the Richard method. The compute interval is 1-120 seconds, the fitting interval is 5-30 seconds.

### Optimization Procedure

The goal of the optimization is to tune the parameters of the unstimulated network so that the signal can generate alpha oscillation and have a high DFA exponent in the alpha band. In order to refine a set of candidate parameters, the parameters were manually adjusted to give a fixed point or limit cycle in the phase plane, whose outputs are able to exhibit bursts or oscillations under the stochastic integration scheme (Table.1).

Next, the refined parameter set including $nsig$, $\sigma$, $c_{ee}$, $c_{ie}$ was used as input, which is further optimized by Bayesian optimization to a critical state. The optimization is done by the Python package Ray[Tune] with the default setting.

In order to promote the model generating an alpha oscillation, we set penalties if the peak of the PSD is in other bands (see Algorithm.1).

### Stimulation

When investigating the pre-stimulus regulation, the stimulation is randomly applied to $n$ vertices on the surface, with $n \in 1, 10, 40, 100, 120, 150, 170$. Each stimulation is a single pulse with a strength of 0.001. In a 1000-second simulation, the vertices will receive a stimulation each 500-1500 ms starting from 750ms. When performing PLF analysis, the 1000s simulation is trimmed into trials based on the stimulation. Each trial contains the signal 750 ms before and after the stimulation.

### Phase-locking factor

The PLF is computed with the script adapted from[6]. The signal was first filtered by an FIR filter, extracted amplitude envelope then trimmed into trials as mentioned above. PLF is defined as the average phase at a time point $t$ after stimulation across all $N$ trials:

$$PLF(t) = \left\| \frac{1}{N} \sum_{i}^{N} z_i(t) \right\| \tag{7}$$

where $z_i$ is the unit vector indicating the phase angle at $t$.

### Pre-stimulus regulation

Pre-stimulus phase regulation is calculated from PLF and the phase 5 ms before stimulation. The range of phase angle, $-\pi$ to $-\pi$, were divided into 32 smaller overlapping ranges, each of which has a range of $\pi \backslash 8$. Trials were sorted into the 32 groups basing on their phase angle 5 ms before the stimulation. Then, PLF at 150 ms was computed for each of the bins. Treating the normalized PLF at 150 ms as a distribution of phase at -5 ms, the phase regulation could be considered as the expectation of the phase angle at -5 ms:

$$Reg_{phase} = \left\| \frac{1}{\sum_i^P PLF_i(150)} \sum_{i}^{P} PLF(150)_i * u_i(-5) \right\| \tag{8}$$

**Algorithm 1** Tuning parameter for the model

**Require:** $nsig \leftarrow generateRandomNumber[0.0001, 0.004]$
**Require:** $\sigma \leftarrow generateRandomNumber[0.2, 0.5]$
**Require:** $c_{ee} \leftarrow generateRandomNumber[8, 18]$
**Require:** $c_{ei} \leftarrow generateRandomNumber[710]$
**Ensure:** minimize *score*
  $p \leftarrow PSDpeak(data)$
  BANDS = [[0.5,4], [4,8], [8,16], [16,30], [30,100]]
  $randomSearchSteps = 150$
  goal=0.85
  **while** $score \geq 0.06$ **do**
    $data \leftarrow model(nsig, \sigma, c_{ee}, c_{ei})$
    **for** $i$ in range(1 to 5) **do**
      $f \leftarrow filter(data, BANDS(i))$
      $DFA_i \leftarrow DFA(f)$
      **if** $p$ in BAND(i) **then**
        $b \leftarrow i$
        $DFA_{band} \leftarrow DFA_i$
      **end if**
    **end for**
    $DFA_{raw} = DFA(data)$
    **if** $DFA_{band} > DFA_{raw}$ **then**
      $DFA \leftarrow DFA_{band}$
    **else**
      $DFA \leftarrow DFA_{raw}$
    **end if**
    **if** $p$ in BANDS(3) **then** ▷ Alpha band
      $score \leftarrow 0.85 - DFA$
    **else if** $p$ in BANDS(2) | BANDS(4) **then**
      $score \leftarrow 0.85 - DFA * 0.92$
    **else if** $p$ in BANDS(1) | BANDS(5) **then**
      $score \leftarrow 0.85 - DFA * 0.87$
     Update $nsig, \sigma, c_{ee}, c_{ei}$ by $Bayesian(randomSearchSteps, score)$
    **end if**
  **end while**

| Parameter | value | Comment |
|---|---|---|
| $ntau$ | 0 | The noise correlation time |
| $\sigma$ | 0.3 | Standard deviation of Gaussian distribution of the multiplicative noise |
| $nsig$ | 0.0004 | Standard deviation of of the multiplicative noise. Denoted as $D$ above |
| $stim_size$ | 90 | |
| $k_e$ | 1.0 | |
| $k_i$ | 2 | |
| $r_e$ | 1.0 | |
| $r_i$ | 1.0 | |
| $c_{ee}$ | 13.25 | Weight of excitatory-excitatory connection. Denoted as $W_{EE}$ above. |
| $c_{ei}$ | 12.5 | Weight of inhibitory-excitatory connection. |
| $c_{ie}$ | 9.23 | Weight of excitatory-inhibitory connection. Denoted as $W_{EI}$ above. |
| $c_{ii}$ | 2.0 | Weight of inhibitory-inhibitory connection. |
| $\tau_e$ | 10.0 | |
| $\tau_i$ | 10.0 | |
| $a_e$ | 1.2 | |
| $b_e$ | 2.2 | |
| $c_e$ | 4.0 | |
| $a_i$ | 0.8 | |
| $b_i$ | 4.0 | |
| $c_i$ | 1.0 | |
| $\theta_e$ | 2.0 | |
| $\theta_i$ | 1.5 | |
| $\alpha_e$ | 0.55 | |
| $\alpha_i$ | 1.0 | |
| $P$ | 2.5 | Constant stimulation to excitatory population in WC model. |
| $Q$ | 0.0 | Constant stimulation to inhibitory population in WC model. |
| shift sigmoid | False | |

**Table 1.** Fixed parameters of the model after optimization

where P is the bins, $u_i$ is the unit vector indicating the phase angle at 5 ms be the stimulation.

When computing the pre-stimulus amplitude regulation, the average amplitude from -150 to -50 ms for each trial was sort into by percentile (Fig.4b,e). The amplitude regulation is defined as the Spearman correlation between the amplitude percentile and PLF at 150ms after stimulation.

## References


1. Shen, W., McKeown, C. R., Demas, J. A. & Cline, H. T. Inhibition to excitation ratio regulates visual system responses and behavior in vivo. *J. Neurophysiol.* **106**, 2285–2302, DOI: 10.1152/jn.00641.2011 (2011). Publisher: American Physiological Society.

2. Beggs, J. M. & Timme, N. Being Critical of Criticality in the Brain. *Front. Physiol.* **3**, 163, DOI: 10.3389/fphys.2012.00163 (2012).

3. Zimmern, V. Why Brain Criticality Is Clinically Relevant: A Scoping Review. *Front. Neural Circuits* **14**, 54, DOI: 10.3389/fncir.2020.00054 (2020).

4. Linkenkaer-Hansen, K., Nikouline, V. V., Palva, J. M. & Ilmoniemi, R. J. Long-range temporal correlations and scaling behavior in human brain oscillations. *The J. Neurosci. The Off. J. Soc. for Neurosci.* **21**, 1370–1377 (2001).

5. Jensen, O. & Mazaheri, A. Shaping Functional Architecture by Oscillatory Alpha Activity: Gating by Inhibition. *Front. Hum. Neurosci.* **4** (2010).

6. Avramiea, A.-E. *et al.* Pre-stimulus phase and amplitude regulation of phase-locked responses are maximized in the critical state. *eLife* **9**, e53016, DOI: 10.7554/eLife.53016 (2020).

7. Ritter, P., Schirner, M., McIntosh, A. R. & Jirsa, V. K. The Virtual Brain Integrates Computational Modeling and Multimodal Neuroimaging. *Brain Connect.* **3**, 121–145, DOI: 10.1089/brain.2012.0120 (2013). Publisher: Mary Ann Liebert, Inc., publishers.

8. Schirner, M. *et al.* Brain simulation as a cloud service: The Virtual Brain on EBRAINS. *NeuroImage* **251**, 118973, DOI: 10.1016/j.neuroimage.2022.118973 (2022).

9. Wilson, H. R. & Cowan, J. D. Excitatory and Inhibitory Interactions in Localized Populations of Model Neurons. *Biophys. J.* **12**, 1–24, DOI: 10.1016/S0006-3495(72)86068-5 (1972).

10. Powanwe, A. S. & Longtin, A. Brain rhythm bursts are enhanced by multiplicative noise. *Chaos (Woodbury, N.Y.)* **31**, 013117, DOI: 10.1063/5.0022350 (2021).

11. Lea-Carnall, C. A., Montemurro, M. A., Trujillo-Barreto, N. J., Parkes, L. M. & El-Deredy, W. Cortical Resonance Frequencies Emerge from Network Size and Connectivity. *PLOS Comput. Biol.* **12**, e1004740, DOI: 10.1371/journal.pcbi.1004740 (2016). Publisher: Public Library of Science.

12. Hardstone, R. *et al.* Detrended Fluctuation Analysis: A Scale-Free View on Neuronal Oscillations. *Front. Physiol.* **3** (2012).

13. Makeig, S. *et al.* Dynamic brain sources of visual evoked responses. *Sci. (New York, N.Y.)* **295**, 690–694, DOI: 10.1126/science.1066168 (2002).

14. Kinouchi, O. & Copelli, M. Optimal dynamical range of excitable networks at criticality. *Nat. Phys.* **2**, 348–351, DOI: 10.1038/nphys289 (2006). Number: 5 Publisher: Nature Publishing Group.

15. Larremore, D. B., Shew, W. L. & Restrepo, J. G. Predicting criticality and dynamic range in complex networks: effects of topology. *Phys. Rev. Lett.* **106**, 058101, DOI: 10.1103/PhysRevLett.106.058101 (2011).

16. Beggs, J. M. The criticality hypothesis: how local cortical networks might optimize information processing. *Philos. Transactions Royal Soc. A: Math. Phys. Eng. Sci.* **366**, 329–343, DOI: 10.1098/rsta.2007.2092 (2008). Publisher: Royal Society.

17. Feany, M. B. Neuropeptide modulation of learning and memory processes. *Rev. Neurosci.* **7**, 151–164, DOI: 10.1515/revneuro.1996.7.2.151 (1996).

18. Lakatos, P., Karmos, G., Mehta, A. D., Ulbert, I. & Schroeder, C. E. Entrainment of Neuronal Oscillations as a Mechanism of Attentional Selection. *Science* **320**, 110–113, DOI: 10.1126/science.1154735 (2008). Publisher: American Association for the Advancement of Science.

19. Bröhl, F., Keitel, A. & Kayser, C. MEG Activity in Visual and Auditory Cortices Represents Acoustic Speech-Related Information during Silent Lip Reading. *eNeuro* **9**, ENEURO.0209–22.2022, DOI: 10.1523/ENEURO.0209-22.2022 (2022).

20. Schirner, M., McIntosh, A. R., Jirsa, V., Deco, G. & Ritter, P. Inferring multi-scale neural mechanisms with brain network modelling. *eLife* **7**, e28927, DOI: 10.7554/eLife.28927 (2018). Publisher: eLife Sciences Publications, Ltd.

21. Roy, D. *et al.* Using the Virtual Brain to Reveal the Role of Oscillations and Plasticity in Shaping Brain's Dynamical Landscape. *Brain Connect.* DOI: 10.1089/brain.2014.0252 (2014).


## Acknowledgements (not compulsory)


I'd like to express my deepest thanks to my supervisor Klaus Linkenkaer-Hansen, who is extremely helpful every time when I was confused about my project. I must also thank my daily supervisor Additya Sharma, previous student Arthur Avramiea, and my colleague Nanda Jafarian for their code and suggestions.